Thermal Science and Engineering (2021) Volume 4 Issue 2
doi:10.24294/tse.v4i2.1522

ORIGINAL RESEARCH ARTICLE

Analysis of the influence of the number of venetian blinds on compact heat exchangers

Alberto Menéndez-Pérez[1*], Rubén Borrajo-Pérez[1], Daniel Sacasas-Suarez[2]

[1] *Universidad Tecnológica de La Habana. Centro de Estudio de Tecnologías Energéticas Renovables, CETER. La Habana, Cuba. E-mail: amenendez@mecanica.cujae.edu.cu*

[2] *Centro de Inmunoensayo, CIE. La Habana. Cuba.*

ABSTRACT

The paper presents a numerical study of compact tube-fin heat exchangers with Venetian blades. The influence of the number of Venetian blades on the thermo-hydraulic characteristics of the exchanger is determined. A 3D numerical model was used in the laminar regime and for a Reynolds number variation, based on the hydraulic diameter between 120 and 1,200. By varying the number of Venetian blinds upstream and downstream of the central Venetian blind, it is determined that, for smaller numbers of Reynolds fins with 2 Venetian blades, the highest heat transfer coefficient is obtained. On the other hand, by increasing the air velocity at the model inlet, better heat transfer results are obtained for geometries with a higher number of Venetian blades.

Keywords: Venetian Fins; Heat Transfer Intensification; Numerical Simulation

ARTICLE INFO

Received: 24 October 2021
Accepted: 3 December 2021
Available online: 14 December 2021

1. Introduction

Venetian blades are a widespread configuration. Each Venetian allows the initiation of a new boundary layer, while at the same time acting as a flow disturbing element. These mechanisms enhance heat transfer and make it possible to reduce the size of the equipment, thus achieving greater compactness. Several studies have been carried out on this type of fin, and new configurations have been experimented with and modeled with the aim of perfecting this geometry[1,2].

Among the extended surfaces, the most commonly used are flat, Venetian, alternating, and corrugated fins and possible combinations of these. Vortex generators have been added to these geometries as heat transfer intensifiers. The behavior of the flows is a decisive aspect in heat transfer, so there are two methods that allow altering the heat transfer patterns, as stated by T'Joen *et al.*[3] These methods are defined as: the main flow alteration method and the introduction of secondary flows. It may be the case that both mechanisms are present. The difference is that in the first method; the main features are manipulated through geometric changes, while in the second method the local flow structure is modified.

Venetian fin models are one of the most advanced intensified extended surfaces and are essentially formed by cutting the metal plate of the fin at intervals and rotating the metal strips from an angle that re-directs the flow[4].

There are combinations of heat exchangers with Venetian fins and elliptical, flat, or circular tubes. Geometries with flat tubes have better fin efficiency than geometries with circular tubes[2]. Venetian fins generally result in high heat transfer values per unit area but generate large pressure drops. The reason why Venetian blades are a complex technique to analyze is due to the fact that they have a number of different geometrical parameters. One of the parameters that distinguish Venetian blinds is the angle of inclination of the Venetian blinds (louvers), for this reason, many authors have been dedicated to investigating and establishing the optimal ranges of these angles[1,2,5].

In heat exchangers with circular or elliptical tubes, longitudinal vortices are generated when the flow passes around the tube and these are called horseshoe vortices. The main characteristic of these is that they generate high heat transfer values in the front zone of the tubes and around the tubes[6,7]. However, the heat transfer behind the tube is poor due to the recirculation of the flow in the dead or rear zone of the tube.

For low Reynolds numbers, the thickness of the boundary layer is such that the Venetian blades are embedded within it, thus forcing the fluid to change the channel through which it flows. As the Reynolds number increases, the flow that changes channel decreases, and the flow that maintains the main direction increases. This is due to the presence of a thinner boundary layer.

Karthik *et al*.[8] conclude, from the study of a water-filled air heating system using Venetian fins with elliptical tubes, that increasing the air inlet velocity produces a greater increase in the overall heat transfer coefficient than that obtained by increasing the mass flow rate of water through the tubes.

Sanders[9] states that most of the studies related to this subject are carried out in two dimensions, thus ignoring the effects created on the surface of the tubes. This is because recent articles have concluded that the analysis of three-dimensional flows close to the tube wall does not influence the performance of the exchanger equipment.

Some authors conclude that by using Venetian blades with different degrees of inclination each, good results can be obtained for small Reynolds values. The study consists of comparisons, varying the inter-fin pitch and the angle of inclination of the Venetian blades for a particular arrangement where the Reynolds number takes values between 100 and 1,000 approximately[1,7,8]. A very interesting fact is that for small values of the inter-fin pitch and large values of the tilt angle, large and strong airflow deviations are achieved.

The Schmidt correlation represents a good analytical model to find the efficiency of flat fins and circular tubes. This method offers an equation for the efficiency based on geometrical parameters and materials, used in experimental studies when it is impossible to obtain the temperatures at the fin wall[10], although this method is valid only when radial heat conduction exists in one dimension.

According to Ameel *et al*.[11], the black box the black box behavior of heat exchangers is commonly analyzed by the Logarithmic Mean Temperature Difference (LMTD) method or by the NTU (Number of Transfer Units) method.

There is research showing that Venetian blinds redirect the airflow in the direction parallel to their own planes[12,13], where visualization of the flow in scaled models is used to reach this conclusion.

Achaichia and Cowell[14] conclude in an investigation that undesired inter-fin flows are caused when the inter-veneer pitch is combined with large inter-veneer spacings and small veneer angles. The above criterion is also supported by Tu *et al*.[15] who state that better results are obtained using geometries with small inter-blade pitches (1.6 mm) and small blade angles of 26°.

Kang *et al*.[16] conclude that the use of Venetian blind arrays and multiple circular tubes produces 10%–15% higher heat transfer performance than using flat tubes for the same volumetric flows and velocities.

Although the literature review shows the existence of multiple studies on this type of fins, there is little information on the influence of the number of Venetian blades on the thermo-hydraulic characteristics of these heat exchangers. Precisely, this work determines the influence of the number of Venetian blades on the heat transferred and the

pressure drop in a Reynolds range between 120 and 1,200.

2. Materials and method

Figure 1 shows a front view of a Venetian blind, presenting, among other things, the angle of inclination of the Venetian blinds and the height of the blinds. The figure corresponds to having fins equal to 2 blinds on either side of the central blind, commonly referred to as redirected blinds.

Table 1 below shows the dimensions of the one and two-row Venetian finned tube models to be studied.

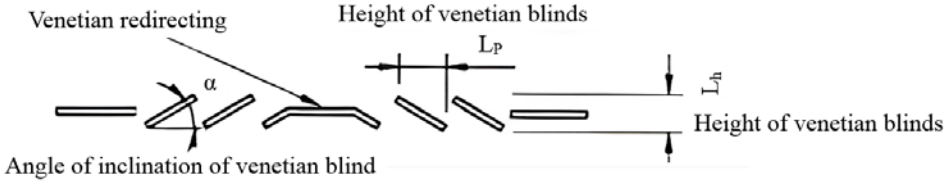

Figure 1. Front view of a venetian blind with a row of tubes.

Table 1. Dimensions of the venetian fin models for one and two rows of circular tubes

Description	Nomenclature	1 row		2 rows	
Pitch between fins [mm]	F_P	1.5			
Fin length [mm]	L	17		34	
Transversal fin spacing [mm]	S_t	22			
Angle of inclination of venetian blind [°]	a	27			
Blade thickness [mm]	t_f	0.1			
Width of venetian blind area [mm]	A_L	9			
Tube radius [mm]	R	4.5			
Distance from flap outlet to channel outlet [mm]	y	60			
Distance from channel inlet to flap inlet [mm]	x	7.5			
Total channel length [mm]	L_C	84		101	
Number of venetian blinds with respect to redirection	C_L	2	3	4	5
Venetian blind pitch [mm]	L_P	1.56	1.15	0.91	0.75
Venetian blind height [mm]	L_h	0.8	0.62	0.43	0.35
Fin Material	Aluminum				

The equations that govern the study of a phenomenon in which the motion of a fluid and its heat exchange with the surfaces it contacts are of interest are the continuity equation, the equations of quantity of motion in each of the axes and the energy equation. These equations in the computational domain, for incompressible flow, with constant properties and in steady state without viscous dissipation and in laminar regime, can be expressed in the same order in which they are mentioned, as follows (equations 1, 2 and 3):

$$\frac{\partial u_i}{\partial x_i} = 0 \tag{1}$$

$$\rho\left[\frac{\partial u_j}{\partial t} + \frac{\partial u_j u_i}{\partial x_j}\right] = -\frac{\partial p}{\partial x_i} - \frac{\partial \tau_{ij}}{\partial x_j} \tag{2}$$

$$c_p\rho\left[\frac{\partial T}{\partial t} + \frac{\partial u_j T}{\partial x_j}\right] = \frac{\partial}{\partial x_j}\left[\lambda\frac{\partial T}{\partial x_j}\right] \tag{3}$$

The solution of equations 1, 2 and 3 is achieved for a computational domain shown in **Figure 2**. The domain, as can be seen, has been extended in the inlet and outlet region of the model. It was extended 7 times the fin spacing in the inlet direction and 7 times the minor diameter of the tube in the outlet direction. The need to have a uniform and one-dimensional velocity profile at the inlet of the model, as well as to avoid the existence of reverse flow in the outlet section is the reason for these extensions.

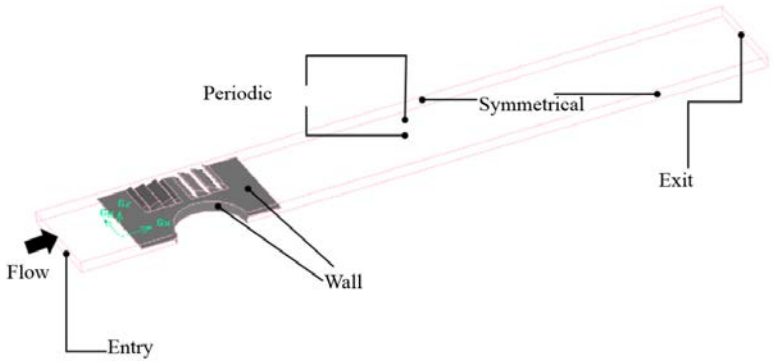

Figure 2. Representation of channel and fin boundary conditions.

The interpolation used for the energy was of the second order upwind type since this is more effective when there is no mesh totally normal to the flow. In the pressure-velocity coupling, the simple method and a first-order upwind scheme were used in the momentum equations and the standard model in the pressure. The fin in the central region of the domain is taken as a solid, while the channels above and below are considered to be fluid regions. Two boundary conditions that are needed are the temperature in the tube and the fluid inlet parameters to the channel. The temperature of the tubes will be considered equal to that of the cooling fluid circulating inside them, so the value of the heat transfer coefficient on the inside of the tube is disregarded given its high value when compared to that which must exist on the outside of the tube. The inlet velocity is data that can vary because the study of different Reynolds numbers requires the change of the velocity at the inlet. The general boundary conditions by region are summarized below:

At model input, equation 4:

$$v = w = 0 \quad u = const. \quad T = const. \tag{4}$$

In the upper and lower part of the domain, periodicity conditions were considered. On the fin surface, in addition to the existence of conjugate heat transfer, there is a no-slip condition, equation 5:

$$u = v = w = 0 \tag{5}$$

On the surface of the tube we will have, equation 6:

$$u = v = w = 0 \quad T = const. \tag{6}$$

$$\frac{\partial u}{\partial y} = \frac{\partial w}{\partial y} = \frac{\partial T}{\partial y} = v = 0 \tag{7}$$

At the model output, equation 8:

$$\frac{\partial u}{\partial x} = \frac{\partial v}{\partial x} = \frac{\partial w}{\partial x} = \frac{\partial T}{\partial x} = 0 \tag{8}$$

The model works under a laminar flow regime with low air velocities in the channel, in anticipation of the existence of annoying kinetic noises. It is also modeled in steady state. The flow to be analyzed is three-dimensional, with the velocity and temperature fields decoupled, which guarantees the independence between both variables. The flow velocity at the model inlet is varied between 0.5 and 5 m/s. The air temperature at the model inlet is 300 K, and at the pipe wall, it is considered equal to 286 K. The flow is considered incompressible.

The geometry and channel region are meshed with hybrid tetrahedron (TGrid) elements in Gambit 2.4.6 software. It has meshed in such a way that the density of elements was able to produce a mesh-independent solution, since the difference between the results of pressure drop and heat transfer coefficient does not exceed 1.6% between two successive mesh sizes. It does not have any element with skewness volumes, nor any element with negative or inverted volume since both would conspire against the convergence of the iterations. For the meshing, size functions were used on the more complex faces, as shown in **Figure 3**.

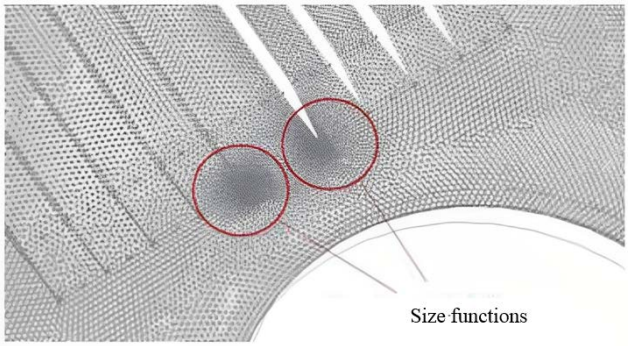

Figure 3. View of the mesh in the fin area where size functions were used.

2.1 Numerical model validation

In order to consider the results valid, the method used for their determination must be certified. The method used here in the certification consists of constructing a computational model with dimensions and characteristics corresponding to one that had already been investigated and its results are available in the literature. The model studied by Han *et al.*[17] was selected and validated against experimental results obtained by Wang *et al.*[18,19] Han *et al*. state that the average deviations of the friction factor (*f*) and Colburn factor (*j*) between their numerical model and their validation based on the experiments of Wang *et al*. are 9.3% and 4.5%, respectively. The authors' experiments were based on a similar venetian fin geometry with elliptical tube but using the venetian blades with variable lengths around the edge of the tube. Another difference is that the air entering the wind tunnel has a temperature of 308 K and the wall temperature of the tubes is 353 K. This study has all the dimensions different from the model studied in this work. The same types of flows, interpolations, boundary conditions and convergence criteria for energy and momentum are used. A coupling between velocity and pressure is also implemented using the SIMPLEC algorithm.

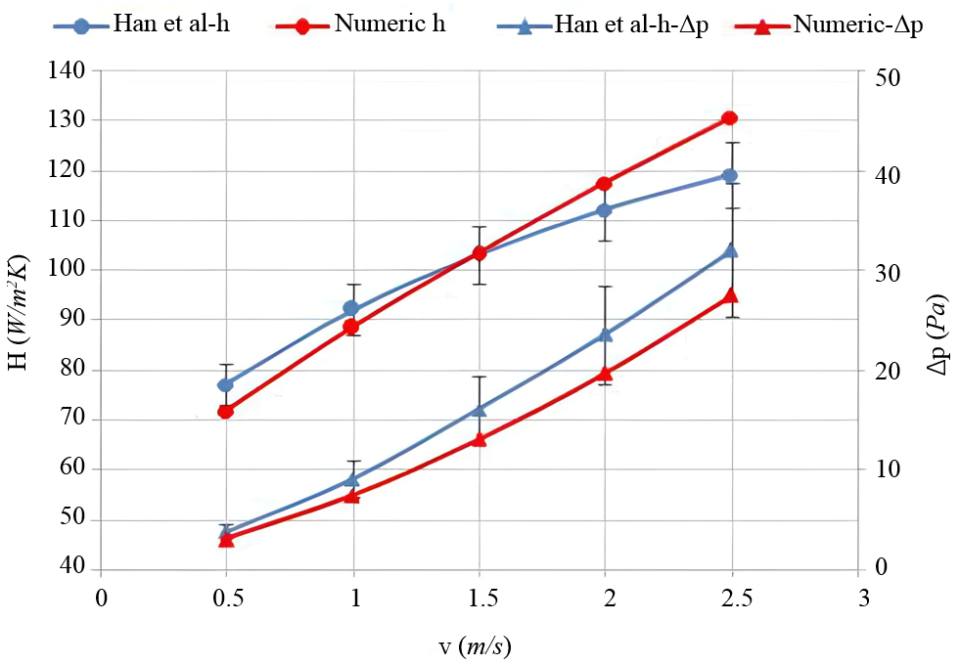

Figure 4. Validation of the global heat transfer coefficient of film and pressure drop.

Figure 4 shows that for the values of Δ*p*, the behavior is quite approximate, although the numerical model slightly underestimates this parameter. The behavior of the heat transfer coefficient is also approximated by the numerical model. The difference between the behaviors of these curves may be caused by the inaccuracy in the reproduction of the geometry shown in the work of Han *et al*., which does not provide the necessary details for the exact reproduction of the model nor the correct constructive form. This work overestimates the value of h for velocities above 1.5 m/s, while underestimates the value of h for velocities below 1.5 m/s when compared to those of Han *et al.*[17].

The average deviations between the results for the global heat transfer film coefficient and the pressure drop of the work of Han *et al.*[17], are of the order of 5.22% and 21.61%, respectively. Then,

despite the differences mentioned above, it can be noted that most of the values are within the uncertainty region, which delimits the error bars in **Figure 4**. In correspondence with the above, we can affirm that the method used in the work to achieve the simulation is valid. It can then be established that the method used, the simplifications, as well as the boundary conditions established in this work are valid to achieve the proposed objectives.

2.2 Data reduction

The Reynolds number was determined using the velocity at the minimum channel section $u_{\min}$, while the characteristic length is the hydraulic diameter of the channel D_h, equation 9:

$$Re = \frac{\rho u_{\min} D_h}{\mu} \tag{9}$$

The heat transferred at the exchange surface can be calculated with the change in air temperature between the inlet and outlet sections of the model ($T_{out} - T_{in}$), the mass flow m_a, and the specific heat of the air c_{pa}, according to equation 10:

$$Q = m_a c_{pa} \left(T_{out} - T_{in} \right) \tag{10}$$

When the fluid undergoes a phase change inside the tubes, it is common practice to consider a high value for the internal film heat transfer coefficient. Assuming this, the overall coefficient will be obtained by considering only the external heat transfer coefficient and the conduction inside the tube wall. The temperature of the internal wall of the tubes is considered constant and with the same value as that of the circulating coolant. The heat transferred can also be calculated through the well-known equation involving the logarithmic ΔT_{ln} (LMTD), knowing the transfer area A_f, the overall transfer coefficient $\bar{h}$, and the aforementioned temperature difference, equation 11:

$$Q_h = \eta_0 \bar{h} A_f F \Delta T_{ln} \tag{11}$$

The LMTD correction factor, F, was considered to be zero because one of the fluids maintains its temperature constant. The global heat transfer coefficient is calculated considering the equality of the heat expressed by equations 10 and 11.

$$Q = Q_h$$

The fin efficiency η_0 is involved and is itself a function of the heat transfer coefficient. The efficiency is calculated as a function of the fin efficiency η and the total transfer area A_0, equation 12:

$$\eta_0 = 1 - \frac{A_f}{A_0}(1 - \eta) \tag{12}$$

The fin efficiency for a rectangular fin is determined using the approximate method developed by Schmidt for circular fins. The fin efficiency is expressed according to equation 13:

$$\eta = \frac{\tanh\left(m r_t \varphi\right)}{\left(m r_t \varphi\right)} \tag{13}$$

The value of m is calculated with the thermal conductivity of the fin (k_f) and its thickness (f_t), equation 14.

$$m = \sqrt{\frac{2\bar{h}}{k_f f_t}} \tag{14}$$

On the other hand, the term φ is obtained with the equivalent tube radius divided by the tube radius. This parameter depends on the geometry of the heat exchanger according to (equation 15 and 16):

$$\varphi = \left(\frac{R_{eq}}{r_t} - 1\right)\left(1 + 0.35\, ln\left(\frac{R_{eq}}{r_t}\right)\right) \tag{15}$$

$$\frac{R_{eq}}{r_t} = 1.27 \frac{X_m}{r_t}\left(\frac{X_L}{X_m} - 0.3\right)^{1/2} \tag{16}$$

Where X_m is half of the transverse spacing and X_L is calculated according to equation 17:

$$X_L = \frac{\sqrt{\left(\frac{S_T}{2}\right)^2 + S_L^2}}{2} \tag{177}$$

The fin efficiency and the global heat transfer

coefficient have an implicit formulation, therefore an iterative process is needed. The equality of heats of equations 10 and 11 is the one that must be satisfied. For a fixed geometry, there is only one pair of values of these magnitudes, fin efficiency and global transfer coefficient, that meet this condition. Then the Colburn factor can be obtained from the Prandtl number and the friction factor according to equation 18:

$$j = \frac{\bar{h}}{\rho_m c_{pa} u_{min}} Pr^{2/3}$$

$$f = \frac{\Delta p}{0.5 \rho_a u_{min}^2} \left(\frac{A_{min}}{A_t}\right) \quad (18)$$

Where A_{min} is the minimum area of the passage section and A_t is the heat transfer area.

3. Results and discussion

The following are the essential elements to discuss the results obtained. The values obtained for the relevant quantities *h*, *Δp*, *j*, *f* and *Q* will be discussed here. These are the indicators generally used to make comparisons between heat exchange surfaces and therefore define which are the best performing surfaces.

It is customary, as mentioned before, in the current literature to present the behavior of heat exchangers using dimensionless numbers and consequently the values of the Colburn factor *j* and the Friction factor *f* as a function of the Reynolds number are shown in **Figure 5** and **Figure 6**. The legend of the figure refers to the number of venetian blades on each side of the central venetian blade, which produces a change of direction in the angle of the blades. Therefore, a number 3 on the scale would mean a total of 6 additional venetian blinds to the central one.

A probable explanation for this phenomenon is that when the number of venetian blades increases, so does the number of surfaces where new boundary layers develop (leading edges of the venetian blades). When the number of venetian blades is lower, they bring the cold fluid flowing through the center of the channel closer to the fin surface. This is possible because the smaller the number of blades, the longer the blades are.

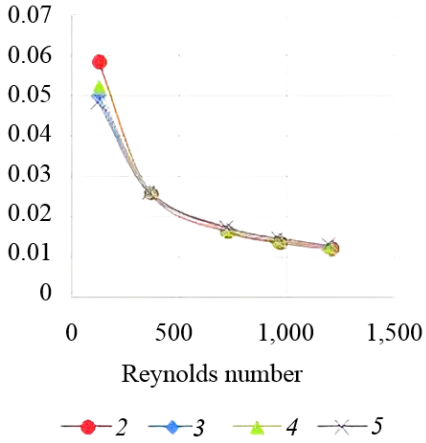

Figure 5. Colburn factor as a function of Reynolds number for two rows of tubes.

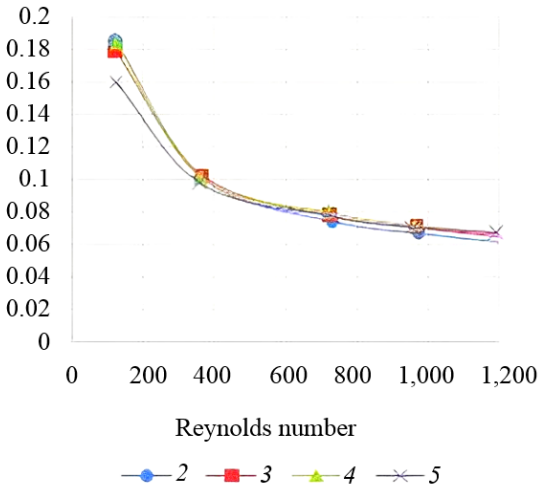

Figure 6. Friction factor as a function of Reynolds number for two rows of pipes.

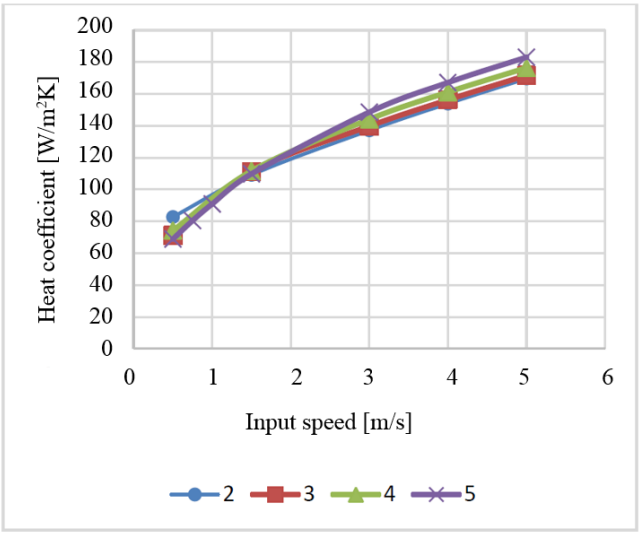

Figure 7. Heat transfer coefficient as a function of inlet velocity for two rows of tubes.

Figure 8 shows that the most important heat transfer mechanism, when velocities are minimal, is

the development of the boundary layer at the front of the fin and the venetian blades, as it can be observed how the venetian blades break the boundary layer of the fluid, which influences the increase of the heat exchanged. In addition, the region of low heat transfer coefficients associated with the dead zone of the tubes is clearly observed. The differences in heat exchanged in the venetian blind region are due to the incidence of the flow on the surfaces of the pipes.

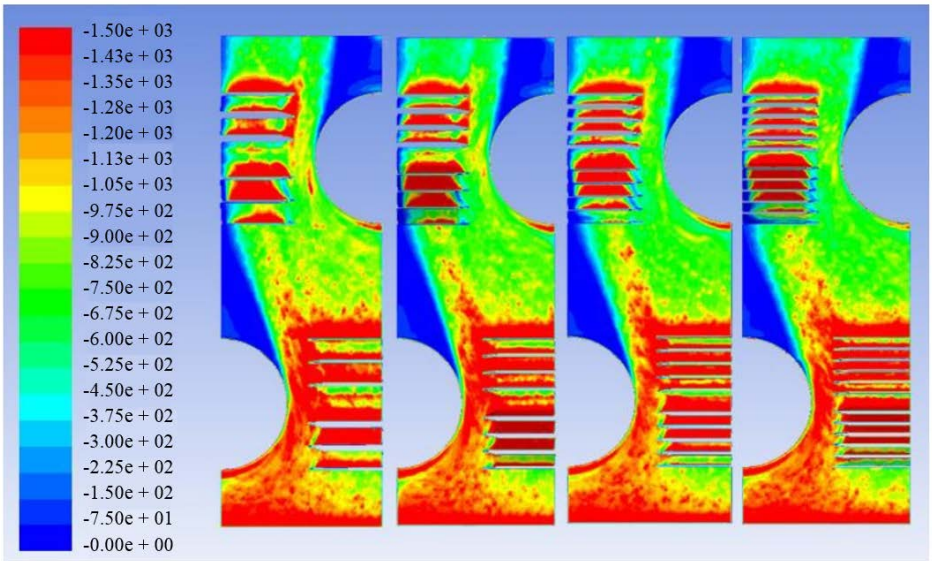

Figure 8. Heat flux in (W/m^2) over the top face of the fin surface for models with C_L between 2 and 5 (from left to right). Velocity of 1.5 m/s from bottom to top.

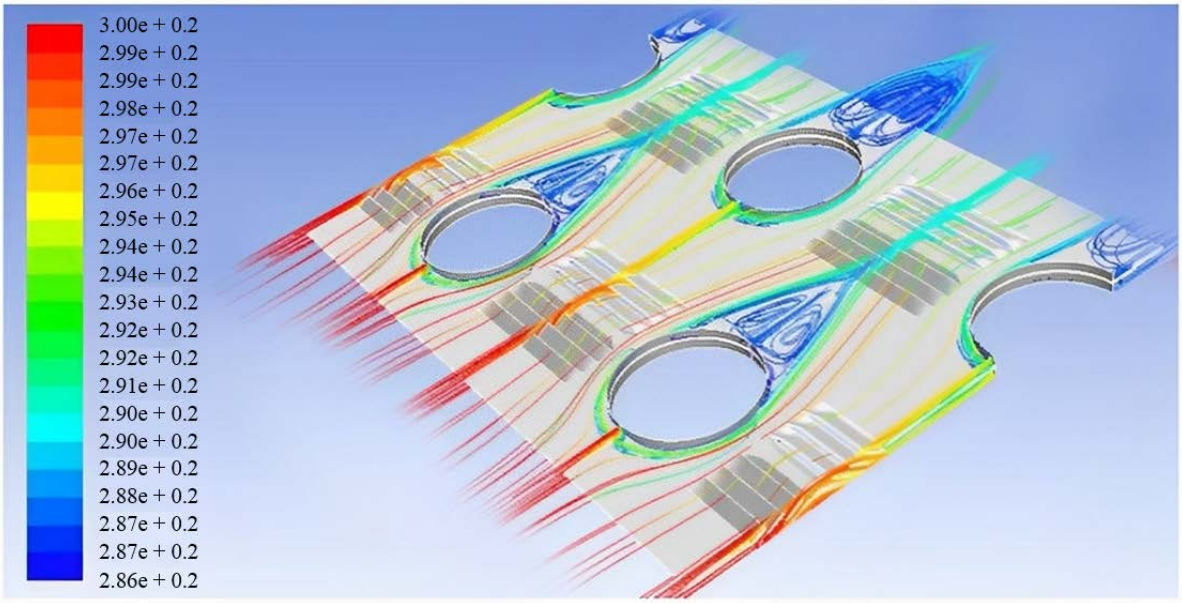

Figure 9. Colored streamlines as a function of temperature in degrees Kelvin. For an inlet velocity of 1.5 m/s.

Figure 9 shows the streamlines generated at the inlet face of the channel for an extension of the symmetry condition of the model. The differences in the horseshoe vortices in the first and second tubes are clearly seen. In the second tube, these vortices tend to contour the tube less, causing a larger recirculation region than that observed behind the tubes in the first row. It is also observed how the acceleration effect that the flow experiences when passing through the second row is manifested, decreasing the recirculation in the rear area of the tube.

Also, **Figure 10** shows the temperature profiles at the top of the fin. The main flow direction is from right to left. It can be observed that as the fluid has a higher velocity at the inlet of the model, the

average temperature of the fin is higher and there is less uniformity at the outlet of the fluid. As this surface is a heat exchanger where the air is at a higher temperature than the fin surface, there is a greater heat transfer, since the temperature difference between the fin surface and the fluid is greater. It is observed at the outlet of the fin that the temperature is never constant over the entire surface, highlighting that the higher the velocity, the greater the temperature gradients.

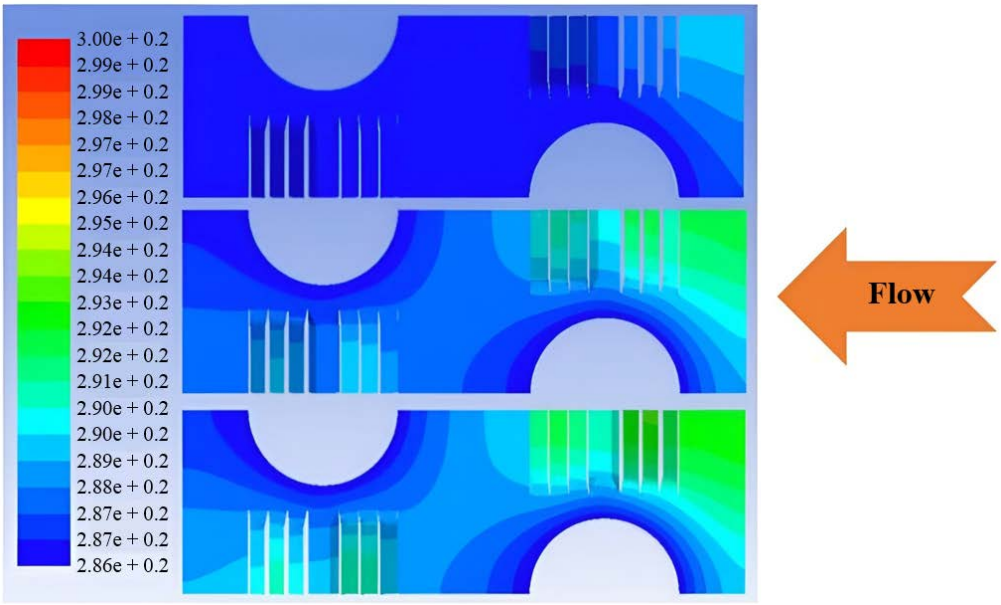

Figure 10. Temperature [K] at the top face of the fin for three inlet velocities, 0.5, 3.0 and 5.0 m/s (from top to bottom).

3.1 Limitations of the work

The results of the work are valid only for fins of similar geometry and in the vicinity of the dimensions of the one studied here, as long as the flow regime is laminar.

4. Conclusions

A computational model capable of reproducing the thermo-hydraulic behavior, shown in the literature consulted, of a heat exchange surface of venetian fins and circular tubes was created. This surface was used as a vehicle for the certification of the method.

Among the fundamental results, it was determined that for the model with two rows of tubes, the flow tends more and more to separate from the lateral face as the velocity increases, while in the first tube the behavior is the opposite, due to the presence of the second tube.

The heat transfer coefficient was found to increase when the number of venetian blades is lower, a result that is accentuated for lower Reynolds numbers. When higher velocities were studied, it was the models with the highest number of venetian blades that presented the best thermal-hydraulic behavior.

Conflict of interest

The authors declare that they have no conflict of interest.

References

1. Wang CC, Chen KY, Liaw JS, *et al*. An experimental study of the air-side performance of fin-and-tube heat exchangers having plain, louver, and semi-dimple vortex generator configuration. International Journal of Heat and Mass Transfer 2015; 80: 281–287.
2. Delač B, Trp A, Lenić K. Numerical investigation of heat transfer enhancement in a fin and tube heat exchanger using vortex generators. International Journal of Heat and Mass Transfer 2014; 78: 662–669.
3. T'Joen C, Huisseune H, Canière H, *et al*. Interaction between mean flow and thermo-hydraulic behaviour in inclined louvered fins. International Journal of Heat and Mass Transfer 2011; 54(4): 826–837.
4. Powar VS, Mirza MM. Performance of louver fin pattern as extended surface used to enhance heat transfer—A review. Int Journal of Engineering Research and Applications, 2013, 3: 1409–1413.
5. Wang CC, Chen KY, Lin YT. Investigation of the

semi-dimple vortex generator applicable to fin-and-tube heat exchangers. Applied Thermal Engineering 2015; 88: 192–197.
6. Zhong Y, Jacobi AM. Experimental study of louver-fin flat-tube heat exchanger performance under frosting conditions. In: Shah RK, Ishizuka M, Ruby TM, *et al.* (editors). Proceedings of the Fifth International Conference on Enhanced, Compact and Ultra-Compact Heat Exchangers: Science, Engineering and Technology; 2005 Sept 11–16; Whistler, British; Columbia, Canada. Hoboken, New Jersey, USA: Engineering Conferences International; 2005.
7. Salviano LO, Dezan DJ, Yanagihara JI. Optimization of winglet-type vortex generator positions and angles in plate-fin compact heat exchanger: Response surface methodology and direct optimization. International Journal of Heat and Mass Transfer 2015; 82: 373–387.
8. Pooranachandran K, Ali KSIL, Narasingamurthi K, *et al*. Experimental and numerical investigation of a louvered fin and elliptical tube compact heat exchanger. Thermal Science 2015; 19(2): 679–692.
9. Sanders PA. Effects of louver lengthand vortex generators to augment tube wall heat transfer in louvered fin heat exchangers [MSc thesis]. Virginia, USA: Virginia Polytechnic Institute and State University; 2005.
10. Huisseune H, T'Joen C, De Jaeger P, *et al*. Influence of the louver and delta winglet geometry on the thermal hydraulic performance of a compound heat exchanger. International Journal of Heat and Mass Transfer 2013; 57(1): 58–72.
11. Ameel B, Degroote J, Huisseune H, *et al*. Interaction effects between parameters in a vortex generator and louvered fin compact heat exchanger. International Journal of Heat and Mass Transfer 2014; 77: 247–256.
12. Schmidt TE. Heat transfer calculations for extended surfaces. Refrigerating Engineering 1949; 57(4): 351–357.
13. Ameel B, Huisseune H, Degroote J, *et al*. On fin efficiency in interrupted fin and tube heat exchangers. International Journal of Heat and Mass Transfer 2013; 60: 557–566.
14. Achaichia A, Cowell TA. Heat transfer and pressure drop characteristics of flat tube and louvered plate fin surfaces. Experimental Thermal and Fluid Science 1988; 1(2): 147–157.
15. Tu X, Lin H, Liang X. CFD simulation and experimental study on air-side performance for MCHX. International Refrigeration and Air Conditioning Conference; 2010 Jul 10–15; Indiana, USA. Purdue University; 2010.
16. Kang H, Jacobi AM, Minkyoo L. Air-side heat transfer performance of louver fin and multi-tube heat exchanger for fuel-cell cooling application, in air-side h eat transfer performance of louver fin and multi-tube heat exchanger for fuel-cell. International Refrigeration and Air Conditioning Conference; 2012 Jul 16–19; Indiana, USA. Purdue University; 2012.
17. Han H, He YL, Li YS, *et al*. A numerical study on compact enhanced fin-and-tube heat exchangers with oval and circular tube configurations. International Journal of Heat and Mass Transfer 2013; 65: 686–695.
18. Wang CC, Lee CJ, Chang CT, *et al*. Some aspects of plate fin-and-tube heat exchangers: With and without louvers. Journal of Enhanced Heat Transfer 1999; 6(5): 357–368.
19. Wang CC, Tsai YM, Lu DC. Comprehensive study of convex-louver and wavy fin-and-tube heat exchangers. Journal of Thermophysics and Heat Transfer 1998; 12(3): 423–430.